

无机化学学报

2017年

第33卷

第7期

目次

综述

钙钛矿型太阳能电池制备工艺及稳定性研究进展.....郭文明 钟敏(1097)

论文

含 C^N-螯合配体的环戊二烯基铈抗癌配合物(英文)

.....路小敏 田梦 田珍珍 田来进 李梦琪 黄静 刘哲(1119)

石墨烯助剂与 Ni(II)活性位点协同增强 TiO₂ 制氢性能.....张超颖 王苹 刘岩岩 胡灵娜(1132)

Co₃O₄/ZnO 修饰针灸针的制备及其在葡萄糖检测领域的应用(英文)

.....苑鸿雯 王玉路 马驰 耿俊隆 张利强 崔海(1139)

溶胶-凝胶法合成 Li_{1-x}Na_xMn₂O₄ 及其作为水系锂离子电池正极材料的电化学性能

.....陶洪亮 米常焕 张迎霞(1147)

高活性固体碱 Na₂O/Al₂O₃-MgO 的合成与表征.....刘守庆 李雪梅 和献武 刘祥义 郑志锋(1153)

层级纳米花环状 Bi₂O₃/(BiO)₂CO₃ 复合材料光催化降解罗丹明 B

.....宋强 李莉 罗鸿祥 刘越 杨长龙(1161)

3,4,5,6-四氟邻苯二甲酸与含氮配体的过渡金属配合物的合成、晶体结构及对 Fe³⁺ 的荧光传感

.....张美娜 郑晓丽 屈相龙 李夏 高源(1172)

复合光催化剂 AgI/AgCl/h-BN 的制备及光催化性能

.....张素云 汪家喜 王迁 柏吉 毕源泉 陆润清 吕晓萌(1181)

过渡金属铁配合物 Fe(CO)_{5-x}(PR₃)_x 的结构与性质的理论研究

.....郭彩红 李海宇 李俊 贾建峰 武海顺(1187)

p-n 异质结 BiPO₄/Ag₃PO₄ 的制备及其增强的模拟太阳光活性

.....王昭华 蔡琼瑶 叶挺铭 郭英娜 耿直 杨霞 于洪斌(1196)

La 和 Zn 掺杂铈酸铋的光催化降解性能及其机理.....许青青 吕亮 叶冬菊 宋锐权(1205)

以不同铜配合物为探针分子的温敏漆制备及性能

.....孙梦婷 陆思宇 孙晶 王媛 于文生 崔思远(1217)

Fe-CuS/还原氧化石墨烯(RGO)的制备及其光催化性能

.....杨明荣 沈勇 胡小赛 张惠芳 王黎明 徐丽慧 邢亚均(1223)

铜/石墨烯复合材料的制备及催化性能.....李娟 赵安婷 邵姣婧 卢丽平(1231)

ZrO₂ 包覆的层状富锂正极材料 0.6Li[Li_{1/3}Mn_{2/3}]O₂·0.4LiNi_{5/12}Mn_{5/12}Co_{1/6}O₂ 的电化学性能

.....黄继春 梅琳 马峥 朱贤雨 全景宾 李德成(1236)

Fe(C₅H₄-CH₂-Trp-OMe)₂ 的合成、晶体结构及金属离子识别性能

.....刘伟 李霞 李银峰 赵金安 吴本来 宋毛平(1243)

- 蒸汽相转化法原位诱导沸石化制备 Y-ZSM-5 双沸石复合物
高禾鑫 李 鹏 杜艳泽 郑家军 潘 梦 刘芝平 李瑞丰(1249)
- 含吡咯环的缩氨基硫脲席夫碱镍、铜配合物的晶体结构及与 DNA 的相互作用(英文)
李晓静 毛盼东 吴伟娜 寇 凯 刘树阳 王 元(1257)
- 金属离子导向合成两个金属配位聚合物:晶体结构和荧光性质(英文)
马德运 李 湘 郭海福 马燕华 林婉纯 温美玲 蔡立文 朱立烽(1266)
- 基于自由基配体的 Dy(III)配合物的设计、合成、结构及磁性(英文)
胡 鹏 肖凤屏 植中强 杜凤翔 邓肖娟 黄国洪 张 森 苏 芬 王莉娜(1273)
- 双 Salamo 型四脒配体构筑的锌(II)配合物:合成,晶体结构和荧光性质(英文)
杨玉华 郝 静 董银娟 王 刚 董文魁(1280)
- 三核钌簇合物 $[\text{PyCH}=\text{C}(\text{Ph})\text{O}]_2\text{Ru}_3(\text{CO})_8$ 的合成、结构及反应性(英文)
马志宏 刘 倩 秦 玫 韩占刚 郑学忠 林 进(1293)
- 一种由 1,4,7-三氮杂环壬烷形成的三脚架配体及其与高氯酸钠组装的含 $[\text{Na}_4(\text{ClO}_4)_4]$ 四面体
 晶体结构(英文).....李秀敏 杨 雨 张宗尧 曹 睿(1299)
- 基于 2,5-噻吩二甲酸的钙(II)和钡(II)配位聚合物的合成、晶体结构及性质(英文)
张雁红 Adhikari Shiba Prasad Day Cynthia Lachgar Abdou(1305)

CHINESE JOURNAL OF INORGANIC CHEMISTRY

Vol.33

No.7

Jul. 2017

CONTENTS

Cover



Potent Cyclopentadienyl Iridium Anticancer Complexes Containing C[^]N-chelating Ligands (English)

LU Xiao-Min, TIAN Meng, TIAN Zhen-Zhen, TIAN Lai-Jin, LI Meng-Qi, HUANG Jing, LIU Zhe

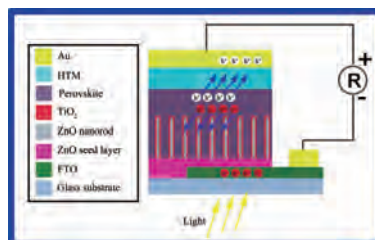
DOI:10.11862/CJIC.2017.155

Chinese J. Inorg. Chem., 2017,33:1119-1131

Reviews

Research Progress on the Preparation Technology and Stability of Perovskite Solar Cells

GUO Wen-Ming, ZHONG Min



Combining with the innovative achievements of Zhong Min's research group on the preparation and performance research of all-solid-state perovskite sensitized solar cells based on ZnO@TiO₂ core-shell structure nanorod arrays, this paper emphatically summarized the preparation technology and optimization of electron transport layer and perovskite layer and also discussed the stability and the prospect of the commercialization of perovskite solar cells.

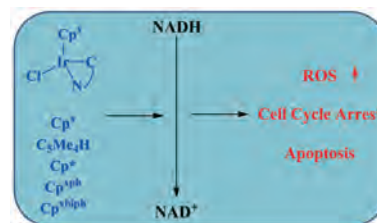
DOI:10.11862/CJIC.2017.152

Chinese J. Inorg. Chem., 2017,33:1097-1118

Articles

Potent Cyclopentadienyl Iridium Anticancer Complexes Containing C[^]N-chelating Ligands (English)

LU Xiao-Min, TIAN Meng, TIAN Zhen-Zhen, TIAN Lai-Jin, LI Meng-Qi, HUANG Jing, LIU Zhe



Half-sandwich cyclopentadienyl iridium complexes containing C[^]N-chelating ligands display potent anticancer activities and are attractive for development as new anticancer agents.

DOI:10.11862/CJIC.2017.155

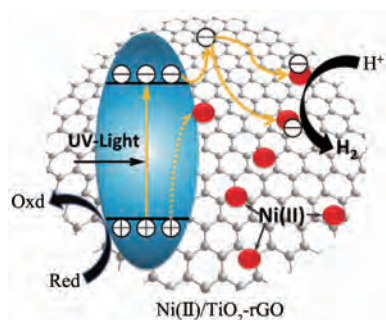
Chinese J. Inorg. Chem., 2017,33:1119-1131

Synergistic Effect of Graphene as Electron-Transfer Mediator and Ni(II) as Interfacial Catalytic Active Site for Enhanced H₂-Production Performance of TiO₂

ZHANG Chao-Ying, WANG Ping, LIU Yan-Yan, HU Ling-Na

DOI:10.11862/CJIC.2017.170

Chinese J. Inorg. Chem., **2017**,**33**:1132-1138



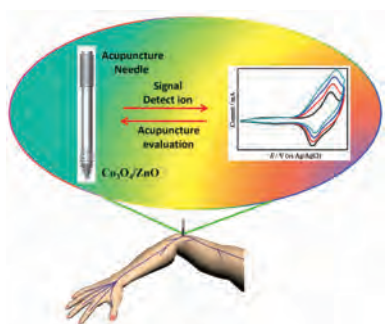
Highly efficient TiO₂ photocatalysts co-modified by reduced graphene oxide (rGO) as electron-transfer mediator and Ni(II) as interfacial catalytic active-site were synthesized via a two-step process including the initial hydrothermal method of rGO on the TiO₂ surface and the following low-temperature impregnation method of Ni(II) on the rGO.

Co₃O₄/ZnO Modified Acupuncture Needle: Preparation and Application in Detecting Glucose (English)

YUAN Hong-Wen, WANG Yu-Lu, MA Chi, GENG Jun-Long, ZHANG Li-Qiang, CUI Hai

DOI:10.11862/CJIC.2017.118

Chinese J. Inorg. Chem., **2017**,**33**:1139-1146



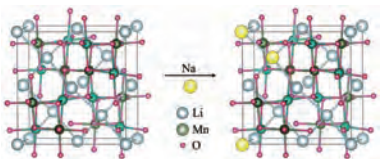
The Co₃O₄/ZnO acicular nanorod arrays (ANRAs) decorated acupuncture needle exhibits a high sensitivity of 2 264.27 $\mu\text{A} \cdot \text{L} \cdot \text{mmol}^{-1} \cdot \text{cm}^{-2}$, a fast response time (<4 s) and a detection limit as low as 0.311 $\mu\text{mol} \cdot \text{L}^{-1}$ ($S/N=3$).

Aqueous Li-Ion Battery Cathode Material Li_{1-x}Na_xMn₂O₄ Prepared by Sol-gel Method and Its Electrochemical Performance

TAO Hong-Liang, MI Chang-Huan, ZHANG Ying-Xia

DOI:10.11862/CJIC.2017.156

Chinese J. Inorg. Chem., **2017**,**33**:1147-1152



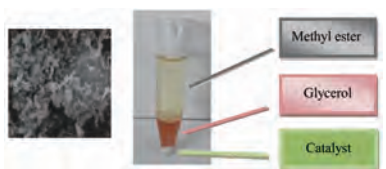
Sodium is doped into the 8a site to replace lithium and sodium can stay in the structure after the material is fully delithiated. This can make the structure more stable and improve cycle performance.

Synthesis and Characterization of Solid Base Catalyst Na₂O/Al₂O₃-MgO with High Activity

LIU Shou-Qing, LI Xue-Mei, HE Xian-Wu, LIU Xiang-Yi, ZHENG Zhi-Feng

DOI:10.11862/CJIC.2017.141

Chinese J. Inorg. Chem., **2017**,**33**:1153-1160



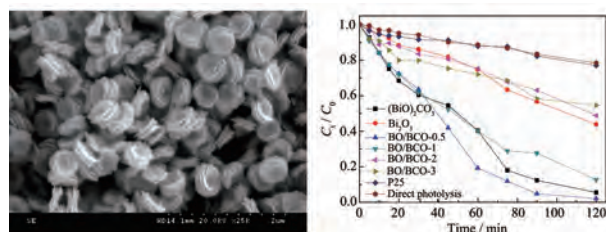
By using the ammonia as precipitator and undergoing impregnation with Na₂CO₃, Na₂O/Al₂O₃-MgO catalyst with hydrotalcite-like structure has been synthesized. The methyl esterification rate of malania oleifera oil is more than 90%.

Hierarchical Nanoflower-Ring Structure Bi₂O₃/(BiO)₂CO₃ Composite for Photocatalytic Degradation of Rhodamine B

SONG Qiang, LI Li, LUO Hong-Xiang, LIU Yue, YANG Chang-Long

DOI:10.11862/CJIC.2017.139

Chinese J. Inorg. Chem., **2017**,**33**:1161-1171



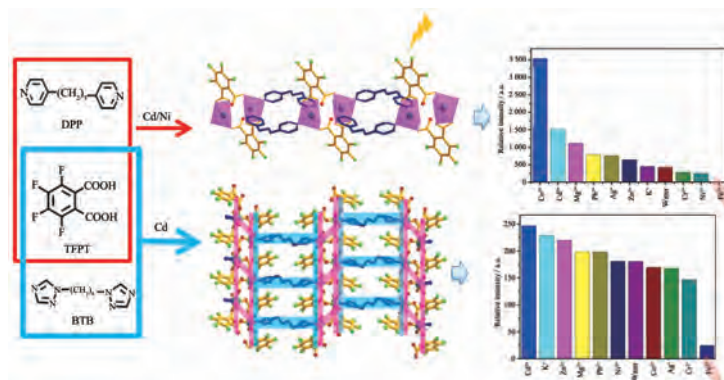
Hierarchical nanoflower-ring structure Bi₂O₃/(BiO)₂CO₃ (BO/BCO) composite was synthesized, and the formation of special morphology led to narrowed band gap and change the reflection and scattering of photoelectrons, which were conducive to the absorption efficiency of light and transferring of photogenerated charges.

Syntheses, Crystal Structures and Fluorescence Sensing for Fe³⁺ of Transition Metal Complexes with 3,4,5,6-Tetrafluorophthalic Acid and N-Donor Ligands

ZHANG Mei-Na, ZHENG Xiao-Li,
QU Xiang-Long, LI Xia, GAO Yuan

DOI:10.11862/CJIC.2017.137

Chinese J. Inorg. Chem., **2017**,**33**:1172-1180

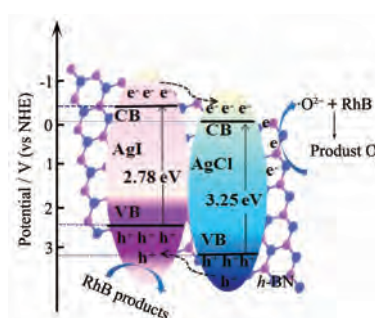


Preparation and Photocatalytic Performance of AgI/AgCl/h-BN Composites

ZHANG Su-Yun, WANG Jia-Xi, WANG Qian,
BAI Ji, BI Yuan-Quan, LU Run-Qing,
LÜ Xiao-Meng

DOI:10.11862/CJIC.2017.146

Chinese J. Inorg. Chem., **2017**,**33**:1181-1186



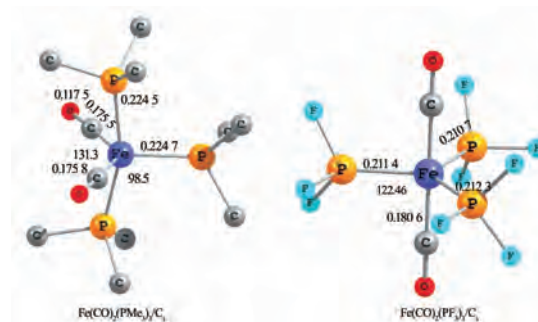
The ternary composite AgI/AgCl/h-BN was synthesized via water-soluble KCl crystal temple and ion-exchange process using *h*-BN nanosheets as support. The obtained composite was obtained with high visible light activity and stability. The result paved the way of potential application of *h*-BN in the field of photocatalyst.

Theoretical Study on Structure and Property of Iron Carbonyl Derivatives Fe(CO)₅₋₃(PR₃)_x

GUO Cai-Hong, LI Hai-Yu, LI Jun,
JIA Jian-Feng, WU Hai-Shun

DOI:10.11862/CJIC.2017.143

Chinese J. Inorg. Chem., **2017**,**33**:1187-1195



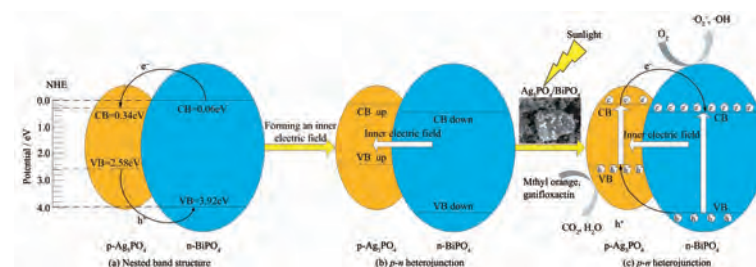
The geometric structures, bonding characteristic, and bond dissociation of iron complexes Fe(CO)₅₋₃(PR₃)_x (x=1~3, R=H, F, Me) were investigated by DFT method. NBO analysis shows that the charge transfer between the phosphorus ligand (s) and iron enhanced the covalent interaction between Fe and CO.

BiPO₄/Ag₃PO₄ p-n Heterojunction with Enhanced Photocatalytic Activity under Simulated Sunlight Irradiation

WANG Zhao-Hua, CAI Qiong-Yao,
YE Ting-Ming, GUO Ying-Na, GENG Zhi,
YANG Xia, YU Hong-Bin

DOI:10.11862/CJIC.2017.140

Chinese J. Inorg. Chem., **2017**,**33**:1196-1204



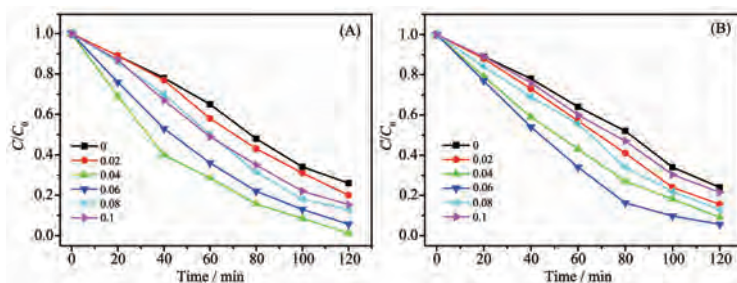
The p-n heterojunction BiPO₄/Ag₃PO₄ exhibits higher degradation and mineralized activities, and the better stability on degradation of methyl orange and gatifloxacin than the single BiPO₄ and Ag₃PO₄.

Photocatalytic Degradation Activity and Mechanism of Niobate Bismuth Nanoparticles Doped with La and Zn

XU Qing-Qing, LÜ Liang, YE Dong-Ju, SONG Kai-Quan

DOI:10.11862/CJIC.2017.134

Chinese J. Inorg. Chem., 2017,33:1205-1216

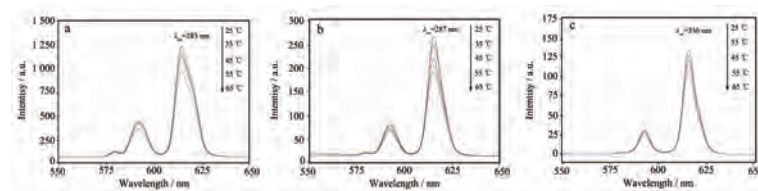


Preparation and Property of Temperature Sensitive Paints with Different Europium Complexes as Probe Molecules

SUN Meng-Ting, LU Si-Yu, SUN Jing, WANG Yuan, YU Wen-Sheng, CUI Si-Yuan

DOI:10.11862/CJIC.2017.000

Chinese J. Inorg. Chem., 2017,33:1217-1222



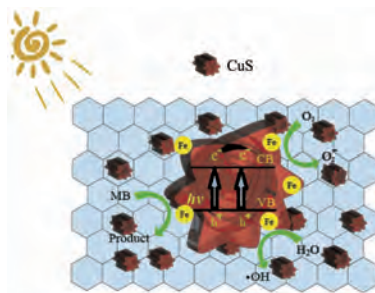
Three kinds of temperature sensitive paint (Eu(MAA)₃Phen/PMMA, Eu(Sal)₃Phen/PMMA and Eu(CA)₃Phen/PMMA) were obtained. It is found that the temperature sensitivity of TSPs is different in different temperature ranges.

Synthesis of Fe-CuS/RGO by Solvothermal Method with High Visible Photocatalytic Activity

YANG Ming-Rong, SHEN Yong, HU Xiao-Sai, ZHANG Hui-Fang, WANG Li-Ming, XU Li-Hui, XING Ya-Jun

DOI:10.11862/CJIC.2017.148

Chinese J. Inorg. Chem., 2017,33:1223-1230



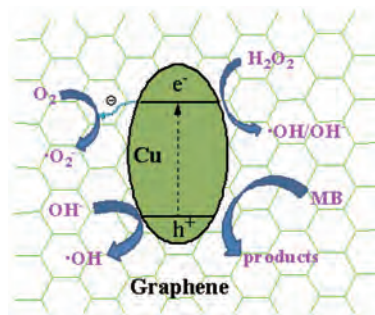
The Fe-CuS/RGO photocatalysts showed enhanced photocatalytic activity for methylene blue solution in comparison with CuS/RGO because Fe element could act as an interfacial charge transfer channel.

Preparation and Catalytic Properties of Copper/Graphene Composites

LI Juan, ZHAO An-Ting, SHAO Jiao-Jing, LU Li-Ping

DOI:10.11862/CJIC.2017.167

Chinese J. Inorg. Chem., 2017,33:1231-1235



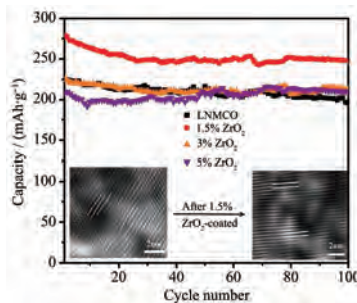
Cu/RGO composites exhibited enhanced catalytic activity toward MB. The dominant contribution is associated with RGO which can act as electron acceptors and transfer channels to enhance the charge separation efficiency, results also indicated that $\cdot\text{O}_2^-$, $\cdot\text{OH}$ and h^+ were critical species in the catalytic reaction. Copper/graphene catalysts have potential applications.

Electrochemical Performance of Li-rich Layered Cathode Material $0.6\text{Li}[\text{Li}_{1/3}\text{Mn}_{2/3}]\text{O}_2 \cdot 0.4\text{LiNi}_{5/12}\text{Mn}_{5/12}\text{Co}_{1/6}\text{O}_2$ by ZrO_2 Coating

HUANG Ji-Chun, MEI Lin, MA Zheng, ZHU Xian-Yu, QUAN Jing-Bin, LI De-Cheng

DOI:10.11862/CJIC.2017.173

Chinese J. Inorg. Chem., 2017,33:1236-1242



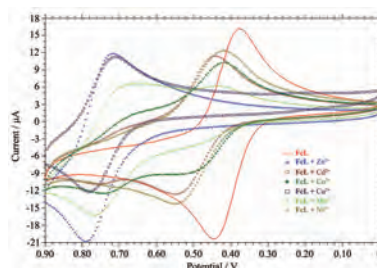
The 1.5% ZrO_2 -coated LNMCO provides a large discharge capacities of $279.3 \text{ mAh} \cdot \text{g}^{-1}$, and $248.3 \text{ mAh} \cdot \text{g}^{-1}$ after 100 cycles, superior to the bare sample at a current density of $20 \text{ mA} \cdot \text{g}^{-1}$ and shown little disordered arrangements of lattice fringes compared with the LNMCO sample after 101 cycles.

Synthesis, Crystal Structure and Electrochemical Metal Cation Recognition Investigation of $\text{Fe}(\text{C}_5\text{H}_4\text{-CH}_2\text{-Trp-OMe})_2$

LIU Wei, LI Xia, LI Yin-Feng, ZHAO Jin-An, WU Ben-Lai, SONG Mao-Ping

DOI:10.11862/CJIC.2017.127

Chinese J. Inorg. Chem., **2017**,**33**:1243-1248



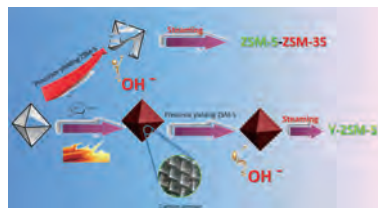
Electrochemical investigations of **FcL** have demonstrated that addition of Zn^{2+} and Cu^{2+} results in large shifts of respective Fe/Fe^+ redox couple to more positive potentials, 342 and 335 mV, respectively, and this suggests that **FcL** has good abilities in recognizing the vital Zn^{2+} and Cu^{2+} .

Y-ZSM-5 Zeolite-Zeolite Composites Prepared by the Steam-Assisted Conversion Method

GAO He-Xin, LI Peng, DU Yan-Ze, ZHENG Jia-Jun, PAN Meng, LIU Zhi-Ping, LI Rui-Feng

DOI:10.11862/CJIC.2017.148

Chinese J. Inorg. Chem., **2017**,**33**:1249-1256



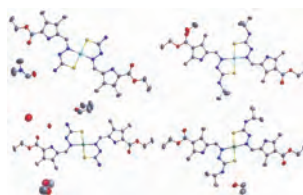
Carbon membrane yielded from glucose alleviates the depolymerization of the frameworks of Y zeolite crystals during the preparation of dry gel and steam-assisted conversion processes, which guarantees the constant composition in the precursors yielding ZSM-5 zeolite, and a zeolite-zeolite composite composed of FAU and MFI crystals was therefore obtained.

Ni(II)/Cu(II) Complexes with Two Pyrrole Thiosemicarbazone Ligands: Crystal Structures and DNA Interaction (English)

LI Xiao-Jing, MAO Pan-Dong, WU Wei-Na, KOU Kai, LIU Shu-Yang, WANG Yuan

DOI:10.11862/CJIC.2017.151

Chinese J. Inorg. Chem., **2017**,**33**:1257-1265



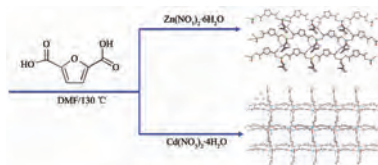
Four complexes $[\text{Ni}(\text{L}^1)_2] \cdot 2\text{DMF}$, $[\text{Cu}(\text{L}^1)_2] \cdot \text{THF} \cdot 0.25\text{MeOH} \cdot 2.25\text{H}_2\text{O}$, $[\text{Ni}(\text{L}^2)_2] \cdot 2\text{MeOH}$ and $[\text{Cu}(\text{L}^2)_2] \cdot 2\text{EtOH}$ with two thiosemicarbazone ligands bearing pyrrole unit have been synthesized and characterized. All complexes can bind to DNA and have potential pharmaceutical activity.

Metal Ions Controlled Assembly of Two Coordination Polymers: Structures and Luminescence Properties (English)

MA De-Yun, LI Xiang, GUO Hai-Fu, MA Yan-Hua, LIN Wan-Chun, WEN Mei-Ling, CAI Li-Wen, ZHU Li-Feng

DOI:10.11862/CJIC.2017.162

Chinese J. Inorg. Chem., **2017**,**33**:1266-1272



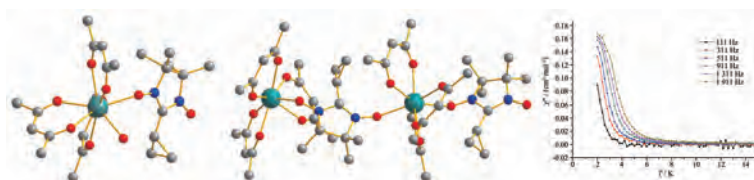
By changing the metal ions, two CPs have been prepared based on the 2,5-furandicarboxylic acid under the same reaction conditions (130 °C) and structural characterized. Moreover, the luminescence properties have also been investigated.

Two Dy(III)-Radical Complexes: Synthesis, Structures and Magnetic Properties (English)

HU Peng, XIAO Feng-Ping, ZHI Zhong-Qiang, DU Feng-Xiang, DENG Xiao-Juan, HUANG Guo-Hong, ZHANG Miao, SU Feng, WANG Li-Na

DOI:10.11862/CJIC.2017.149

Chinese J. Inorg. Chem., **2017**,**33**:1273-1279



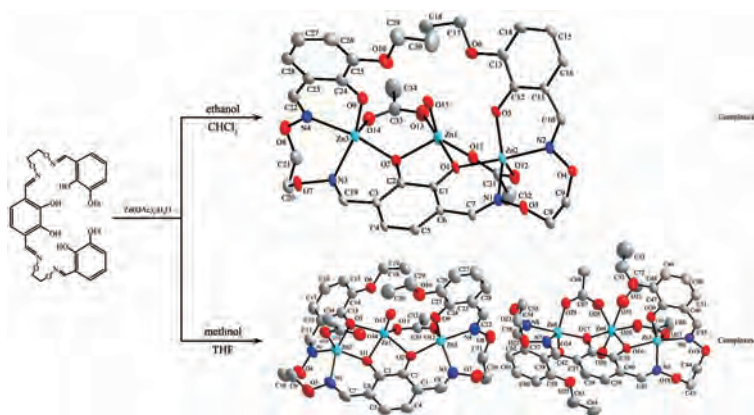
The figure shows the molecular structures of two Dy(III)-radical complexes. The structures are depicted as ball-and-stick models, showing the coordination of the Dy(III) ions to the radical ligands. To the right, a plot shows the magnetic susceptibility χ (emu/mol) versus temperature T (K) for the complexes. The plot shows a sharp increase in susceptibility at low temperatures, indicating magnetic ordering.

Two Zn(II) Complexes Constructed from a Bis(salamo)-type Tetraoxime Ligand: Syntheses, Crystal Structures and Luminescence Properties (English)

YANG Yu-Hua, HAO Jing, DONG Yin-Juan, WANG Gang, DONG Wen-Kui

DOI:10.11862/CJIC.2017.150

Chinese J. Inorg. Chem., **2017**,**33**:1280-1292

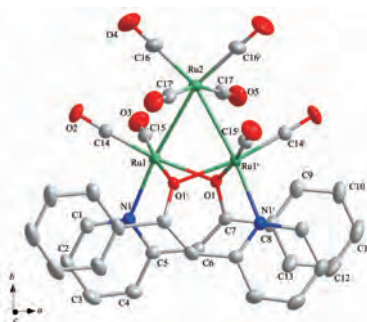


Synthesis, Structure and Reactivity of a Trinuclear Ruthenium Cluster Compound [PyCH=C(Ph)O]₂Ru₃(CO)₈ (English)

MA Zhi-Hong, LIU Qian, QIN Mei, HAN Zhan-Gang, ZHENG Xue-Zhong, LIN Jin

DOI:10.11862/CJIC.2017.135

Chinese J. Inorg. Chem., **2017**,**33**:1293-1298



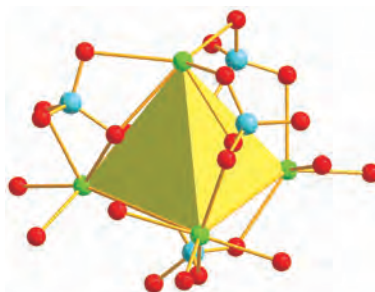
Thermal treatment of PyCH₂COPh with Ru₃(CO)₁₂ in refluxing toluene gave a new trinuclear ruthenium cluster compound [PyCH=C(Ph)O]₂Ru₃(CO)₈. Reactions of this compound with cyclopentadiene or indene show that the coordination properties of cyclopentadiene and indene are higher than that of pyridine alcohol.

A Tripodal Tris-tacn (tacn=1,4,7-Triazacyclononane) Ligand and Its Ability to Assemble a [Na₄(ClO₄)₄] Tetrahedron Cluster (English)

LI Xiu-Min, YANG Yu, ZHANG Zong-Yao, CAO Rui

DOI:10.11862/CJIC.2017.144

Chinese J. Inorg. Chem., **2017**,**33**:1299-1304



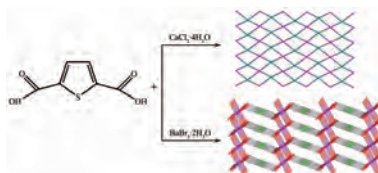
Novel tripodal ligands derived from tris(xylyl)amine backbone assemble a [Na₄(ClO₄)₄] tetrahedron cluster with C₃ symmetry.

Syntheses, Crystal Structures and Characterization of Ca(II) and Ba(II) Coordination Polymers Derived from Thiophene-2,5-dicarboxylate (English)

ZHANG Yan-Hong, Adhikari Shiba Prasad, Day Cynthia, Lachgar Abdou

DOI:10.11862/CJIC.2017.158

Chinese J. Inorg. Chem., **2017**,**33**:1305-1312



Two new alkaline earth metal coordination polymers [Ca(tdc)(DMF)₂]_n (**1**) and [Ba(tdc)]_n (**2**) (H₂tdc=2,5-thiophene dicarboxylate) have been synthesized. Complex **1** exhibits a two-dimensional (2D) layer structure, whereas complex **2** features a 3D framework. Both the two complexes exhibit strong fluorescent properties at room temperature.